THE JOURNAL OF BIOLOGICAL CHEMISTRY VOL. 290, NO. 41, pp. 24715–24726, October 9, 2015

Snf1 Phosphorylates Adenylate Cyclase and Negatively Regulates Protein Kinase A-dependent Transcription in *Saccharomyces cerevisiae*[*]

Received for publication, April 13, 2015, and in revised form, August 25, 2015 Published, JBC Papers in Press, August 26, 2015, DOI 10.1074/jbc.M115.658005

Raffaele Nicastro[‡§1], **Farida Tripodi**[‡§1], **Marco Gaggini**[‡§], **Andrea Castoldi**[‡§], **Veronica Reghellin**[‡§2], **Simona Nonnis**[¶‖], **Gabriella Tedeschi**[¶‖], **and Paola Coccetti**[‡§3]

From the [‡]*Department of Biotechnology and Biosciences, University of Milano-Bicocca, 20126 Milan, Italy,* [§]*SYSBIO, Centre of Systems Biology, 20126 Milan, Italy,* [¶]*Dipartimento di Patologia Animale, Igiene e Sanità Pubblica Veterinaria-Biochemistry, University of Milano, 20133 Milan, Italy, and the* [‖]*Filarete Foundation, 20139 Milan, Italy*

Background: The Snf1/AMPK and PKA pathways are crucial for nutrient sensing and utilization in yeast.
Results: A novel cross-talk mechanism between Snf1/AMPK and PKA is proposed.
Conclusion: Snf1 and Cyr1 interact in a nutrient-independent manner. Active Snf1 phosphorylates Cyr1 and negatively regulates cAMP content and PKA-dependent transcription.
Significance: This is the first evidence of regulation of PKA pathway by Snf1/AMPK.

In eukaryotes, nutrient availability and metabolism are coordinated by sensing mechanisms and signaling pathways, which influence a broad set of cellular functions such as transcription and metabolic pathways to match environmental conditions. In yeast, PKA is activated in the presence of high glucose concentrations, favoring fast nutrient utilization, shutting down stress responses, and boosting growth. On the contrary, Snf1/AMPK is activated in the presence of low glucose or alternative carbon sources, thus promoting an energy saving program through transcriptional activation and phosphorylation of metabolic enzymes. The PKA and Snf1/AMPK pathways share common downstream targets. Moreover, PKA has been reported to negatively influence the activation of Snf1/AMPK. We report a new cross-talk mechanism with a Snf1-dependent regulation of the PKA pathway. We show that Snf1 and adenylate cyclase (Cyr1) interact in a nutrient-independent manner. Moreover, we identify Cyr1 as a Snf1 substrate and show that Snf1 activation state influences Cyr1 phosphorylation pattern, cAMP intracellular levels, and PKA-dependent transcription.

All organisms need to match growth and metabolism with the availability of nutrients. In the budding yeast *Saccharomyces cerevisiae*, several mechanisms of sensing of the carbon source present in the environment have evolved (see Refs. 1–3 for extensive review). Nutrients, and in particular glucose, influence the yeast cell metabolic behavior through the activation of signaling pathways, which in turn finely tune transcription and enzymatic activities (4), as well as cell growth and cell cycle (5).

The main signaling pathway activated by glucose in yeast is the PKA pathway, which shows extensive involvement in growth, proliferation, and metabolism (2, 6). The second messenger responsible for the activation of PKA is cAMP, which is synthesized by adenylate cyclase (Cyr1) upon stimulus from the G-proteins Gpa2 and the RAS pathway (1, 7). cAMP binds to a homodimer of PKA regulatory subunits Bcy1, causing its dissociation from the dimer of catalytic subunits (composed by two of the partially redundant proteins Tpk1, Tpk2, and Tpk3), thus activating the kinase (8). Active PKA has a broad influence on transcription. During exponential growth and in the absence of stress, PKA phosphorylates the transcription factors Msn2,4, thus causing their confinement to the cytoplasm (9). Msn2,4 activate the transcription of genes with promoters containing stress response element sequences, comprising genes coding for chaperones, antioxidant proteins, and proteases and, more in general, for elements necessary to respond to various stress types (10). Besides Msn2,4, PKA controls several other transcription factors including Rim15 (11) and Rap1 (12). Furthermore, PKA directly regulates important metabolic pathways such as glycolysis (6). It phosphorylates proteins catalyzing key enzymatic steps, such as both isoforms of pyruvate kinase, Cdc19 and Pyk2 (13–15).

On the contrary, the signaling pathway centered on the kinase Snf1 is required to adapt to nutrient limitation and to utilize alternative carbon sources, such as sucrose or ethanol (16). Snf1 shares evolutionary conserved functions with the AMP-activated kinase (AMPK)[4] in higher eukaryotes, constituting the well defined family of regulators of cellular energy homeostasis in eukaryotes (17). Snf1 is activated through the phosphorylation of Thr^{210} by one of the three constitutively active upstream kinases Sak1, Tos3, and Elm1 (18, 19). In

* This work was supported by grants from the Italian Government and from the Ministero dell'Istruzione, dell'Università e della Ricerca (MIUR)-funded SysBioNet project of the Italian Roadmap for European Strategy Forum on Research Infrastructures Research Infrastructures (to P. C.). The authors declare that they have no conflicts of interest with the contents of this article.
[1] Supported by fellowships from MIUR.
[2] Supported by a fellowship from SysBioNet.
[3] To whom correspondence should be addressed: Dept. of Biotechnology and Biosciences, University of Milano-Bicocca and SYSBIO, Centre of Systems Biology, Piazza della Scienza 2, 20126 Milan, Italy. Tel.: 390264483521; E-mail: paola.coccetti@unimib.it.

[4] The abbreviations used are: AMPK, AMP-activated kinase; RAD, RAS-associating domain.

TABLE 1
Yeast strains used in this work

Strain	Genotype	Origin
BY wt[a]	*MATa his3Δ1 leu2Δ0 met15Δ0 ura3Δ0*	Open Biosystems
Snf1Δ[a]	*MATa his3Δ1 leu2Δ0 met15Δ0 ura3Δ0 snf1::HPH*	Ref. 25
Snf1−9myc[a]	*MATa his3Δ1 leu2Δ0 met15Δ0 ura3Δ0 SNF1-9myc:LEU2*	This study
Cyr1-TAP[a]	*MATa his3Δ1 leu2Δ0 met15Δ0 ura3Δ0 CYR1-TAP:HIS3*	Open Biosystems
Snf1-myc Cyr1-TAP[a]	*MATa his3Δ1 leu2Δ0 met15Δ0 ura3Δ0 SNF1-9myc:LEU2 CYR1-TAP:HIS3*	This study
Snf1-myc Cyr1-TAP reg1Δ[a]	*MATa his3Δ1 leu2Δ0 met15Δ0 ura3Δ0 SNF1-9myc:LEU2 CYR1-TAP:HIS3 reg1::URA3*	This study
Snf1-HA Cyr1-TAP[a]	*MATa his3Δ1 leu2Δ0 met15Δ0 ura3Δ0 Snf1::HPH [pRS316-SNF1-HA] CYR1-TAP:HIS3*	This study
Snf1-K84R-HA Cyr1-TAP[a]	*MATa his3Δ1 leu2Δ0 met15Δ0 ura3Δ0 Snf1::HPH [pRS316-SNF1-K84R-HA] CYR1-TAP:HIS3*	This study
Snf1Δ [pRS316][b]	*MATa leu2-3,112 ura3-1 trp1-1 his3-11,15 ade2-1 can1-100 snf1::HPH [pRS316]*	This study
Snf1-HA[b]	*MATa leu2-3,112 ura3-1 trp1-1 his3-11,15 ade2-1 can1-100 snf1::HPH [pRS316-SNF1-HA]*	This study
Snf1-G53R-HA[b]	*MATa leu2-3,112 ura3-1 trp1-1 his3-11,15 ade2-1 can1-100 snf1::HPH [pRS316-SNF1-G53R-HA]*	This study
Snf1-K84R-HA[b]	*MATa leu2-3,112 ura3-1 trp1-1 his3-11,15 ade2-1 can1-100 snf1::HPH [pRS316-SNF1-K84R-HA]*	This study
Snf1-T210A-HA[b]	*MATa leu2-3,112 ura3-1 trp1-1 his3-11,15 ade2-1 can1-100 snf1::HPH [pRS316-SNF1-T210A-HA]*	This study
*cyr1Δ pde1Δ yak1*Δitsup;b	*MATa leu2-3,112 ura3-1 trp1-1 his3-11,15 ade2-1 can1-100 cyr1::KanMX, pde2::TRP1, yak1::LEU2 [YCplac33]*	Ref. 56
cyr1Δ pde1Δ yak1Δ Cyr1[b]	*MATa leu2-3,112 ura3-1 trp1-1 his3-11,15 ade2-1 can1-100 cyr1::KanMX, pde2::TRP1, yak1::LEU2 [YCplac33-CYR1]*	This study
mig1Δ [a]	*MATa his3Δ1 leu2Δ0 met15Δ0 ura3Δ0 mig1::KanMX4*	Euroscarf
pde1Δpde2Δsnf1Δ [pRS313][b]	*MATa leu2-3,112 ura3-1 trp1-92 his3-11,15 ade2-1 can1-100 pde1::TRP1 pde2::URA3 snf1::HPH [pRS313]*	This study
pde1Δpde2Δsnf1Δ Snf1-HA[b]	*MATa leu2-3,112 ura3-1 trp1-92 his3-11,15 ade2-1 can1-100 pde1::TRP1 pde2::URA3 snf1::HPH [pRS313-SNF1-HA]*	This study
pde1Δpde2Δsnf1Δ Snf1-G53R-HA[b]	*MATa leu2-3,112 ura3-1 trp1-92 his3-11,15 ade2-1 can1-100 pde1::TRP1 pde2::URA3 snf1::HPH [pRS313-SNF1-G53R-HA]*	This study
cyr1Δ pde1Δ yak1Δ Cyr1-4E[b]	*MATa leu2-3,112 ura3-1 trp1-1 his3-11,15 ade2-1 can1-100 cyr1::KanMX, pde2::TRP1, yak1::LEU2 [YCplac33-CYR1*^{S435E,S527E,T631E,S645E}*]*	This study

[a] Isogenic to BY4741.
[b] Isogenic to W303-1A.

response to high glucose concentrations, Snf1 is inactivated through dephosphorylation of Thr^{210} by the Glc7 protein phosphatase (also known as PP1), which is targeted to Snf1 by the adaptor subunit Reg1 (20, 21). However, recent studies highlighted Snf1 function also in glucose-repressed conditions, as well as its partial activation and its role in the regulation of cell cycle (22–25). The most studied function of Snf1 is the regulation of transcription, involving more than 400 genes (26). Active Snf1 causes the translocation to the cytoplasm of the inhibitor Mig1, responsible for the repression of over 90 genes (27). Besides Mig1, Snf1 regulates the activity of various transcription factors. Cat8 and Sip4, which bind carbon source response elements, mostly regulate the expression of gluconeogenic genes (28), and are activated by Snf1-dependent phosphorylations (29, 30). Furthermore, Snf1 regulates through phosphorylation several metabolic enzymes, such as Pfk27, Gpd2, and Acc1 (6), to promote carbon saving in conditions of nutrient scarceness.

In *S. cerevisiae*, several examples of cross-talk between the Snf1 and PKA pathways have been reported. PKA phosphorylates and contributes to the regulation of the Snf1-activating kinase Sak1 (31) and the β subunit Sip1, preventing the localization of the Snf1 complex to the vacuole (32). Snf1 and PKA share common downstream targets. PKA phosphorylates and deactivates Adr1, the transcriptional activator of several glucose repressed genes, whereas Snf1 indirectly causes its dephosphorylation and activation (33, 34). Surprisingly, both PKA and Snf1 act as repressors of the transcription factor Msn2, but, whereas PKA is the main regulator of this factor, Snf1 targets it only to shut off transcription of the stress response element regulon after prolonged stationary phase (9, 35, 36). Remarkably, a direct regulation of the Snf1 orthologue AMPK by PKA has been demonstrated in human adipocytes, where PKA phosphorylates Ser^{173} of AMPK preventing the phosphorylation of residue Thr^{172}, requested for activation (37). Both residues are conserved in *S. cerevisiae* (Thr^{210} and adjacent Ser^{211}), thus a similar mechanism has been hypothesized in yeast (31).

Here, we propose a novel cross-talk mechanism between Snf1/AMPK and PKA pathways. Seeking for new Snf1 targets, we identify adenylate cyclase (Cyr1) as a Snf1-interacting protein. We show that Cyr1 is a Snf1 target *in vitro* and that its phosphorylation pattern is altered *in vivo* in the *snf1Δ* mutant compared with the wild type. Strikingly, we demonstrate that constitutive activation of Snf1 reduces cAMP intracellular content and functionally impairs PKA activity as a regulator of glucose-repressed genes.

Experimental Procedures

Yeast Strains and Growth Conditions—S. cerevisiae strains used in this study are listed in Table 1. Synthetic medium contained 2, 5, or 0.05% glucose or 2% ethanol (as indicated in the figures), 6.7 g/liter of yeast nitrogen base (Difco), 50 mg/liter of required nutrients at standard pH (5.5).

Cell density of liquid cultures grown at 30 °C was determined with a Coulter counter on mildly sonicated and diluted samples or spectrophotometrically at 600 nm. All experiments were performed with cells in exponential phase of growth, at cell densities between $A_{600\ nm} = 0.1$ (2×10^6 cells/ml) and $A_{600\ nm} = 0.7$ (1.3×10^7 cells/ml).

Recombinant and Genetic Techniques—DNA manipulation and yeast transformations were carried out according to standard techniques. To obtain the tagged strains, proteins were tagged with a C-terminal 4HA or 9myc epitope by an in locus 3′ in-frame insertion. *Escherichia coli DH5α* and *BL21 (DE3)[pLysE]* were used in cloning experiments and for expression of recombinant proteins, respectively. The HpaI-XhoI

fragment of *CYR1* from the YCplac33-CYR1 plasmid (38) was cloned in the HincII-XhoI site of *pIVEX2.4a* plasmid, originating plasmid pIVEX-CYR1(335–1066). Mutant *CYR1-4E (S435E,S527E,T631E,S645E)* gene was obtained by synthesis of a custom HpaI-XhoI CYR1 fragment (Eurofins) and subcloning in the YCplac33-CYR1 plasmid.

Protein Extraction, Immunoblotting, and Immunoprecipitation—Samples of cells were harvested and lysed using ice-cold lysis buffer (50 mM Tris, pH 7.5, 150 mM NaCl, 0.1% Nonidet P-40, 10% glycerol) plus 1 mM PMSF, proteases inhibitor mix (Complete EDTA free protease inhibitor mixture tablets; Roche), and phosphatase inhibitor mix (Sigma). An equal volume of acid-washed glass beads (Sigma) was added, and cells were broken by 20 vortex/ice cycles of 1 min each. Extracts were transferred to new tubes and clarified by centrifugation. Protein concentration was determined using the Bio-Rad protein assay. Crude protein extracts were incubated 2 h at 4 °C with anti-HA affinity matrix (Roche) to immunoprecipitate Snf1-HA protein complexes or with IgG-agarose beads (Sigma) to immunopurify Cyr1-TAP. The immunocomplexes obtained after removal of supernatants were washed three times with lysis buffer and once with 25 mM MOPS, pH 7.5. SDS sample buffer was then added to the beads, and the samples were heated for 5 min at 95 °C. Western blot analysis was performed using anti-TAP antibody (1:2500; Thermo Scientific, Open BioSystems), anti-HA antibody (1:1000, 12CA5; Roche), anti-myc antibody (1:1000, 9E10; Santa Cruz), anti-Cyr1 antibody (1:1000, yC-20, Santa Cruz), and anti-Swi6 (1:1000, kindly provided by L. Breeden). For the analysis of Snf1 interactors, Snf1-HA protein complexes were immunopurified from 270 mg of total protein extract and resolved by SDS-PAGE followed by staining with GelCode™ blue stain reagent (Pierce) for MS analysis. Bands were excised and treated as reported in the section "Sample Preparation and Mass Spectrometry Techniques." For the analysis of Cyr1 phosphorylation, Cyr1-TAP was immunopurified from 9 mg of total protein extract and resolved by SDS-PAGE followed by silver staining, according to the manufacturer's instructions (GE Healthcare).

Recombinant Protein Purification—E. coli strain *BL21 (DE3)[pLysE]* was transformed with pIVEX2.4a-CYR1(335–1066) or pH_{13}-MIG1 (39), cultured in Luria-Bertani broth with 100 mg/liter of ampicillin and 34 mg/liter of chloramphenicol at 37 °C ($A_{600\,nm} = 0.3$), and induced for 2 h with 1 mM isopropyl thio-β-D-galactoside at 30 °C. His_6-Cyr1(335–1066) and His_{13}-Mig1(207–413) were purified on Ni^{2+}-nitrilotriacetic acid beads (Qiagen) and eluted serially with 200, 400, and 800 mM imidazole. Protein concentration was measured by Bradford method using Bio-Rad protein assay kit (Bio-Rad). The purified proteins were dialyzed against a buffer containing 20 mM HEPES, pH 7, 100 mM NaCl, 0.5 mM EDTA, 0.5 mM DTT, 5 mM MgAc, 5% glycerol and stored at −80 °C.

In Vitro Phosphorylation Assays—In vitro phosphorylation of recombinant His_{13}-Mig1(207–413) was carried out as in Ref. 39. *In vitro* phosphorylation of recombinant His_6-Cyr1(335–1066) (4 μg of purified protein) was performed in a buffer containing 20 mM HEPES, pH 7, 100 mM NaCl, 0.5 mM EDTA, 0.5 mM DTT, 5 mM MgAc, using protein kinase Snf1-HA or Snf1-T210A-HA immunopurified from yeast cells growing in 2% glucose. The reaction was started by adding 0.24 μM [γ-^{32}P]ATP (specific radioactivity, 2000 cpm/pmol) and incubated at 30 °C for 30 min. The reaction was stopped by adding 4× SDS sample buffer and then heated for 5 min at 95 °C, and proteins were separated by SDS-PAGE. Phosphorylated bands were visualized by autoradiography.

Sample Preparation and Mass Spectrometry Techniques—The protein content of IP Snf1-HA sample and IP untagged control sample were resolved by SDS-PAGE, analyzed, and compared using a GS-800™ densitometer and Quantity One® analysis software. Each protein band was quantified by densitometric analysis. Only bands exclusively present on IP Snf1-HA sample or bands whose *A* value differed at least 0.1 in the comparison between IP Snf1-HA sample and IP untagged control sample were excised and analyzed by mass spectrometry. These data generate the list of Snf1-interacting proteins reported in Table 2.

Bands were excised after staining, reduced with DTT, and alkylated with 55 mM iodoacetamide at room temperature for 45 min. Bands were dried, soaked with ammonium bicarbonate 0.1 M, and digested overnight with trypsin sequence grade, at 37 °C using a protease: protein ratio (1:10). Tryptic digests were extracted with 50% acetonitrile (ACN) in 0.1% TFA, desalted/concentrated on a μZipTipC18 (Millipore), and analyzed by mass spectrometry. LC-electrospray ionization-MS/MS analysis was performed on a Dionex UltiMate 3000 HPLC System with a PicoFrit ProteoPrep C18 column (200 mm, internal diameter of 75 μm) (New Objective). Gradient: 1% ACN in 0.1% formic acid for 10 min, 1–4% ACN in 0.1% formic acid for 6 min, 4–30% ACN in 0.1% formic acid for 147 min, and 30–50% ACN in 0.1% formic for 3 min at a flow rate of 0.3 μl/min. The eluate was electrosprayed into an LTQ Orbitrap Velos (Thermo Fisher Scientific) through a Proxeon nanoelectrospray ion source (Thermo Fisher Scientific). Data acquisition was controlled by Xcalibur 2.0 and Tune 2.4 software (Thermo Fisher Scientific). The LTQ-Orbitrap was operated in positive mode in data-dependent acquisition mode to automatically alternate between a full scan (m/z 350–2000) in the Orbitrap (at resolution, 60,000; AGC target, 1,000,000) and subsequent CID MS/MS in the linear ion trap of the 20 most intense peaks from full scan (normalized collision energy of 35%, 10-ms activation). Data Base searching was performed using the Sequest search engine contained in the Proteome Discoverer 1.1 software (Thermo Fisher Scientific). The following parameters were used: 10 ppm for MS and 0.5 Da for MS/MS tolerance, carbamidomethylation of Cys as fixed modification; oxidation of Met and phosphorylation of Ser, Tyr, and Thr, as variable modifications, trypsin (two misses) as protease. To generate the list of phosphosites reported in Table 3, we considered only the sites with the highest X Correlation value (Xcorr) in Sequest (≥1.5), the rank value of 1 and the best fragmentation pattern, selected manually after visual inspection of the MS/MS spectra. Three different tools for phosphorylation site prediction where applied: NetPhos Yeast 1.0, NetPhosK 1.0 Server-CBS, and Phosida.

cAMP Assay—cAMP was measured using the cAMP Biotrak EIA Assay (GE Healthcare) following the manufacturer's instructions. Sample preparation was carried out as in Ref. 40.

TABLE 2
Identified Snf1 interactors

Interactor	Description	Previously identified	Sequence coverage	Peptides matched
			%	
Snf1 complex				
Sip1	One of three β subunits of the Snf1 kinase complex	Yes	39.9	18
Sip2	One of three β subunits of the Snf1 kinase complex	Yes	51.6	16
Gal83	One of three β subunits of the Snf1 kinase complex	Yes	54.7	20
Snf4	Activating γ subunit of the AMP-activated Snf1p kinase complex	Yes	76.4	24
Sak1	Upstream serine/threonine kinase for the SNF1 complex	Yes	35.6	30
Reg1	Regulatory subunit of type 1 protein phosphatase Glc7p	Yes	39.4	27
Glucose metabolism				
Cdc19	Pyruvate kinase	No	48.8	14
Hxk2	Hexokinase isoenzyme 2	Yes	18.4	7
Pfk1	α subunit of heterooctameric phosphofructokinase	No	38.3	20
Pfk2	β subunit of heterooctameric phosphofructokinase	Yes	44.9	11
Tdh2	Glyceraldehyde-3-phosphate dehydrogenase, isozyme 2	No	79.2	21
Tdh3	Glyceraldehyde-3-phosphate dehydrogenase, isozyme 3	No	38.5	12
Pdc1	Major of three pyruvate decarboxylase isozymes	No	47.6	14
Eno2	Enolase II	No	78.7	24
Ald6	Cytosolic aldehyde dehydrogenase	No	62.8	26
Atp2	β subunit of the F1 sector of mitochondrial F1F0 ATP synthase	No	58.9	17
Tal1	Transaldolase, enzyme in the nonoxidative pentose phosphate pathway	No	45.7	13
Ribosomes and translation				
Rps8a	Protein component of the small (40S) ribosomal subunit	No	35.5	5
Rpl1a	Ribosomal 60S subunit protein L1A	No	67.1	18
Rpl3	Ribosomal 60S subunit protein L3	No	53.8	21
Rpl4a	Ribosomal 60S subunit protein L4A	No	48.3	13
Rpl6a	Ribosomal 60S subunit protein L6A	No	17.1	2
Rpl8a	Ribosomal 60S subunit protein L8A	Yes	60.9	17
Rpl17b	Ribosomal 60S subunit protein L17B	No	8.7	1
Rpp0	Conserved ribosomal protein P0 of the ribosomal stalk	No	43.6	12
Eft1	Elongation factor 2, also encoded by EFT2	No	37.0	10
Eft2	Elongation factor 2, also encoded by EFT1	No	62.7	41
Tef1	Translational elongation factor EF-1α, also encoded by TEF2	No	23.9	4
Tef2	Translational elongation factor EF-1α, also encoded by TEF1	Yes	63.8	21
Sro9	Cytoplasmic RNA-binding protein; associates with translating ribosomes	Yes	24.7	7
Cft1	RNA-binding subunit of the mRNA cleavage and polyadenylation factor	No	35.0	28
Nip1	eIF3c subunit of the eukaryotic translation initiation factor 3 (eIF3)	No	22.2	13
Stm1	Protein required for optimal translation under nutrient stress	Yes	42.5	12
Amino acid biosynthesis and transport				
Lys20	Homocitrate synthase isozyme	No	61.2	20
Lys21	Homocitrate synthase isozyme	No	47.5	19
Cpa2	Large subunit of carbamoyl phosphate synthetase	No	50.1	37
Npr1	Protein kinase that stabilizes several plasma membrane amino acid transporters	Yes	58.7	28
Fatty acid synthesis				
Fas1	β subunit of fatty acid synthetase	Yes	47.0	66
Fas2	α subunit of fatty acid synthetase	No	52.5	70
IMP dehydrogenases				
Imd1	Nonfunctional protein with homology to IMP dehydrogenase	No	30.6	8
Imd2	Inosine monophosphate dehydrogenase	No	45.3	18
Imd3	Inosine monophosphate dehydrogenase	No	42.2	15
Imd4	Inosine monophosphate dehydrogenase	No	42.8	16
Chaperones				
Ssa2	ATP-binding protein involved in protein folding and vacuolar import of proteins	Yes	64.8	30
Ssb1	Cytoplasmic ATPase that is a ribosome-associated molecular chaperone	Yes	49.8	21
Ssb2	Cytoplasmic ATPase that is a ribosome-associated molecular chaperone	Yes	49.8	21
Bmh1	14-3-3 protein, major isoform	Yes	58.4	13
Others				
Cyr1	Adenylate cyclase, required for cAMP production and protein kinase A signaling	No	19.7	19
Cka1	α catalytic subunit of CK2	Yes	31.3	3
Cop1	α subunit of COPI vesicle coatomer complex	No	26.2	20

Results

Snf1 Interacts with Adenylate Cyclase—Snf1 is known to regulate glucose metabolism and to promote the utilization of alternative carbon sources mainly through the derepression of a large transcription regulon and the phosphorylation of metabolic enzymes (16). However, because the cellular metabolic behavior could be the result of the action of different and somehow opposite signaling pathways, we wondered whether Snf1 could directly regulate such pathways. To detect possible new targets of Snf1, we chose to use a co-immunoprecipitation/MS approach, immunoprecipitating myc-tagged Snf1 and detecting co-immunoprecipitated proteins with mass spectrometry after resolution with SDS-PAGE. We performed this experiment with protein extracts of exponentially growing cells in 2% glucose, because we already demonstrated that in this condition Snf1 is at least partially functional (22, 25).

Interestingly, we identified a total of 50 potentially interacting proteins of which only 16 have been already identified as Snf1 interactors (Fig. 1*A* and Table 2) (41–43). We detected most of the components of the complex of Snf1 and of the Snf1

TABLE 3
Identified phosphopeptides

Sequence	P site (s)	WT	*snf1*Δ	Modification(s)	WT Xcorr	WT *m/z* Da	WT MH^+ Da	WT Charge	*snf1*Δ Xcorr	*snf1*Δ *m/z* Da	*snf1*Δ MH^+ Da	*snf1*Δ Charge	Predicted phosphosites: NetPhos Yeast	Predicted phosphosites: NetPhos K	Predicted phosphosites: Phosida
^{17}QEEQEQQIEQSSPTEANDR^{35}	Ser^{28}	×	×	Ser^{28} (phospho)	2.62	775.9883	2325.9503	3	4.73	775.9901	2325.9558	3	Ser^{28}		
^{17}QEEQEQQIEQSSTPEANDR^{35}	Thr^{30}	×	×	Thr^{30} (phospho)	3.11	775.9844	2325.9386	3	4.21	775.9915	2325.9598	3			
^{210}KPSKDSTLSNHLADNVPSTLR^{230}	Ser^{218}	×	×	Ser^{218} (phospho)	1.77	787.3881	2360.1496	3	2.07	787.3915	2360.1599	3	Ser^{218}		
^{210}KPSKDSTLSNHLADNVPSTLR^{230}	Thr^{228}		×	Thr^{228} (phospho)					1.52	814.0579	2440.1590	3		Thr^{228} (score, 0.91)	
^{281}SFLLGSTSSSSSRR^{294}	Thr^{287}	×	×	Thr^{287} (phospho), Ser^{291} (phospho)	2.18	816.3436	1631.6799	2	4.03	816.3461	1631.6849	2		Ser^{291} (score, 0.77)	Thr^{287}
^{281}SFLLGSTSSSSSRR^{294}	Ser^{288}, Ser^{291}	×	×	Ser^{288} (phospho), Ser^{291} (phospho)	3.83	816.3447	1631.6822	2	3.97	816.3461	1631.6849	2	Ser^{288}	Ser^{291} (score, 0.77)	
^{346}SEKVTPEYNENIPENSNSDNKR^{367}	Thr^{350}	×	×	Thr^{350} (phospho)	1.76	882.0539	2644.1471	3	4.13	882.0574	2644.1576	3	Thr^{350}		
^{368}EATTPTIETPISCKPSLFR^{386}	Thr^{370}	×	×	Thr^{370} (phospho), Cys^{380} (carbamidomethyl)	3.02	743.3613	2228.0692	3	2.57	1114.5403	2228.0733	2			
^{432}KSVSMADLSVAAAAPNGEFTSTSNDR^{457}	Ser^{435}	×		Ser^{435} (phospho)	6.01	1353.6072	2706.2071	2					Ser^{435}		
^{483}SRRSSIDADELDPMSPGPPSK^{503}	Ser^{483}, Ser^{497}	×	×	Ser^{483} (phospho), Ser^{497} (phospho)	2.68	801.3379	2401.9991	3	2.23	801.3417	2402.0105	3	Ser^{483}, Ser^{497}		
^{483}SRRSSIDADELDPMSPGPPSK^{503}	Ser^{497}	×	×	Ser^{497} (phospho)	1.76	774.6774	2322.0176	3	1.51	774.6856	2322.0423	3	Ser^{497}		
^{513}KDNESMVTAGDSNSSFVDICK^{533}	Ser^{524}	×	×	Ser^{524} (phospho), Cys^{532} (carbamidomethyl)	6.11	1192.4935	2383.9798	2	5.90	1192.4950	2383.9827	2			Ser^{524}
^{513}KDNESMVTAGDSNSSFVDICK^{533}	Ser^{527}	×		Ser^{527} (phospho), Cys^{532} (carbamidomethyl)	6.29	1192.4958	2383.9844	2					Ser^{527}		
^{629}KFTSSSVNMNSPDGAQSSGLLLQDEK^{654}	Thr^{631}	×		Thr^{631} (phospho)	3.06	940.7603	2820.2662	3							
^{629}KFTSSSVNMNSPDGAQSSGLLLQDEK^{655}	Ser^{645}	×		Thr^{631} (phospho)	3.15	940.7603	2820.2662	3							Ser^{645}
^{1041}NMTSLTLNKAQLSSIPGELLTK^{1062}	Thr^{1043}, Thr^{1046}, Ser^{1053}		×	Thr^{1043} (phospho), Thr^{1046} (phospho), Ser^{1053} (phospho), Ser^{1054} (phospho)					2.33	670.5564	2679.2038	4	Thr^{1046} (score, 0.81)		Ser^{1053}, Ser^{1054}
^{1097}NKLEYIPPELSQLK^{1110}	Tyr^{1101}, Ser^{1107}		×						1.57	611.2991	1831.8828	3			Ser^{1107}
^{1203}LESITTELYLSGNK^{1221}	Ser^{1211}		×						1.58	773.8703	1546.7333	2			
^{1303}SFISHDIDADLSDLTWLPQLK^{1323}	Ser^{1306}	×	×	Ser^{1306} (phospho)	1.80	803.0618	2407.1707	3	1.52	803.0770	2407.2165	3			Ser^{1306}
^{1380}FRGNDDECLLCLHDSKNQNADYGHNISR^{1407}	Ser^{1394}	×	×	Cys^{1388} (carbamidomethyl), Cys^{1391} (carbamidomethyl)	4.14	857.8657	3428.4411	4	2.91	857.8685	3428.4523	4			Ser^{1394}
^{1656}LQPEISPPTGNLAMVFTDIK^{1675}	Ser^{1661}	×	×	Ser^{1661} (phospho)	1.52	751.04	2251.10	3	1.63	835.0750	2503.2105	3	Ser^{1661}		
^{1739}LLDAQWPEETSVQDGCQVTDR^{1760}	Ser^{1750}	×		Ser^{1750} (phospho), Cys^{1755} (carbamidomethyl)	2.64	880.7224	2640.1527	3							Ser^{1750}

pathway (Fig. 1*B* and Table 2). Remarkably, we identified many new Snf1 potential interactors involved in protein synthesis, such as components of the large ribosomal subunit, and in important metabolic processes, such as glycolytic enzymes (Fig. 1*B* and Table 2).

Strikingly, one of the newly identified interactors was adenylate cyclase (Cyr1), the essential enzyme responsible for the synthesis of cAMP, activator of PKA (Fig. 1 and Table 2). To validate the interaction, we performed co-immunoprecipitation experiments, clearly detecting myc-tagged Snf1 in Cyr1-TAP immunocomplexes (Fig. 2*A*). Moreover, the interaction was not indirectly caused by Snf1 and Cyr1 being common substrates of the phosphatase complex Reg1-Glc7, because it was detectable also in extracts from *reg1*Δ cells (Fig. 2*B*). Interestingly, the interaction was not dependent on the glucose concentration nor the carbon source (Fig. 2, *C* and *D*) and was detectable in the presence of a catalytic-deficient mutant Snf1, Snf1-K84R, or in the presence of a constitutively active mutant Snf1-G53R (Fig. 2*E*). Furthermore, switching bait and prey proteins and detecting Cyr1-TAP in Snf1-HA immunocomplexes, we were able to demonstrate that the interaction was particularly stronger in the presence of a Snf1-K84R mutant (Fig. 2*F*). This finding was of particular interest, because it was previously shown that in glucose-repressed conditions, the catalytic-deficient Snf1 mutant interacts more strongly than the WT with Mig1, a well known Snf1 substrate (44). Taken together, these data demonstrate the physical interaction of Snf1 with Cyr1 and support the possibility of adenylate cyclase being a substrate of Snf1.

Loss of Snf1 Causes an Alteration in the Phosphorylation Pattern of Adenylate Cyclase—Cyr1 is a phosphoprotein, and several phosphorylated residues have been identified in proteomic studies (45–48). Moreover, the sequence of Cyr1 presents five phosphorylatable residues (Ser^{241}, Ser^{554}, Thr^{736}, Ser^{1594}, and Ser^{1978}), two of which were identified as phosphosites *in vivo*, that are contained in perfect Snf1 phosphorylation consensus motifs (Ser^{241} and Ser^{554}). Remarkably, Ser^{241} has been recently identified as being phosphorylated in a Snf1-dependent fashion (24). However, no specific function until now has been assigned to any phosphorylation site.

Because the physical interaction with Snf1 suggested Cyr1 as a possible target of the kinase, we investigated whether the presence or the absence of Snf1 could influence the phosphorylation status of adenylate cyclase *in vivo*. We therefore immunoprecipitated TAP-tagged Cyr1 from WT and *snf1*Δ cell extracts and, after resolution on SDS-PAGE and silver staining, identified the phosphorylated residues by MS analysis (Fig. 3, *A* and *B*, and Table 3). Remarkably, in a WT strain we identified 19 phosphosites, of which only 7 were previously reported, providing an extensive map of adenylate cyclase phosphorylation. Strikingly, a subset of these phosphosites, almost completely localized in the region flanking the RAS-associating domain, turned out to be Snf1-dependent, not being detectable in the *snf1*Δ strain. Surprisingly, none of these sites was one of the five contained in Snf1 consensus sequences discussed above. Interestingly, we also identified seven additional phosphosites that were exclusively present in a *snf1*Δ strain, which could be dependent on kinases normally inhibited by Snf1 (Fig. 3*A*). When

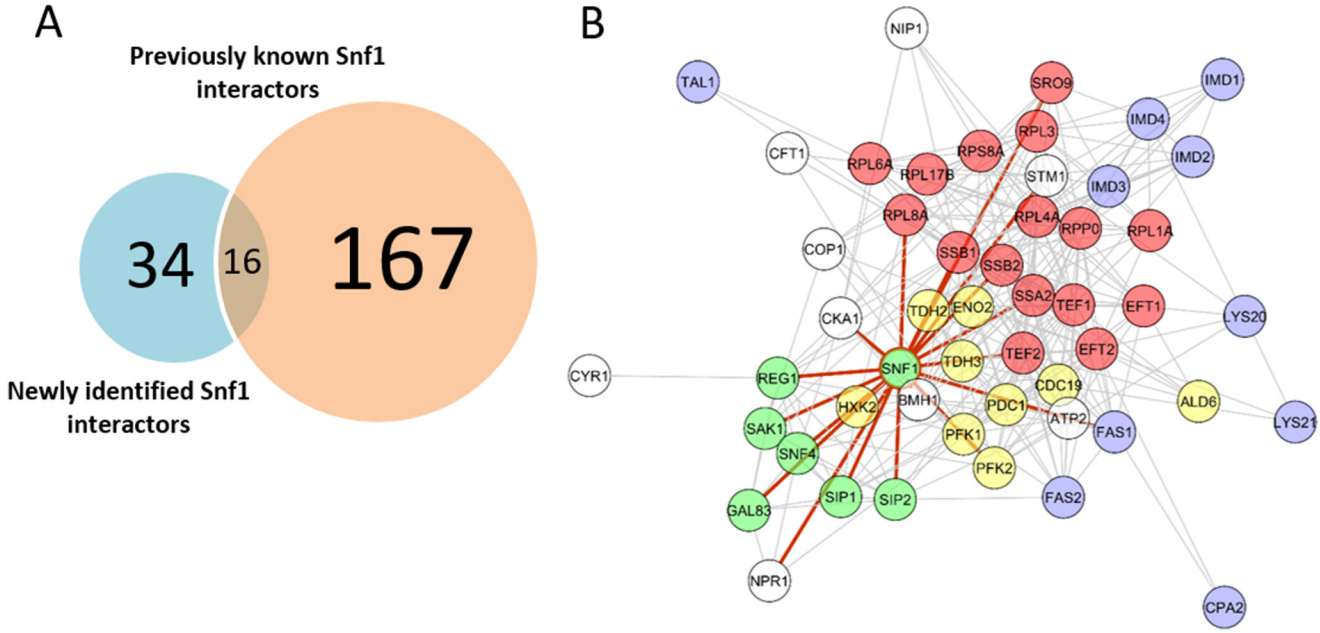

FIGURE 1. **Data analysis of the identified Snf1 interactors.** *A*, intersection between the already known Snf1 physical interactors and the interactors identified in this study. *B*, Gene Ontology Biological Process enrichment analysis of the Snf1 physical interactors in 2% glucose. *Green nodes* indicate proteins of the Snf1 pathway, *yellow nodes* indicate proteins involved in glucose metabolism, *red nodes* indicate proteins involved in the translation process, and *blue nodes* indicate proteins involved in other metabolic processes. *Red edges* indicate previously known interactions, and *gray edges* represent physical interactions between all the nodes. The known interactions were retrieved in the BioGRID database of physical interactions (updated to July 2015). Data visualization was performed with Cytoscape.

we checked whether the identified sites were contained in consensus sequences of a specific kinase, we failed to identify any obviously responsible for the phosphorylation events. These data provide a substantial advance in mapping possible regulatory post-translational modifications of adenylate cyclase and demonstrate the necessity of Snf1 to preserve the proper phosphorylation pattern of Cyr1.

Snf1 Phosphorylates the RAS-associating Domain of Adenylate Cyclase in Vitro—Because we demonstrated that a lack of Snf1 could influence the phosphorylation pattern of Cyr1 *in vivo*, we sought for direct kinase activity of Snf1 on adenylate cyclase *in vitro*. Because we wanted to demonstrate a direct kinase activity of immunopurified Snf1, discerning from phosphorylation events dependent on kinases that co-immunoprecipitate with Snf1 (Table 2), we searched for the most suitable catalytic-deficient mutant of Snf1 to be included as a control. We therefore tested different Snf1 mutants for their ability to phosphorylate recombinant Mig1 *in vitro*. Strikingly, the unphosphorylatable mutant Snf1-T210A turned out to be more impaired than the Snf1-K84R mutant (Fig. 4*A*) and was chosen as a control for subsequent analysis. We then purified from *E. coli* a His_6-tagged region of Cyr1 containing the whole RAS-associating domain (RAD), four of five (Ser^{435}, Ser^{527}, Thr^{631}, and Ser^{645}) residues whose phosphorylation was found to be Snf1-dependent (Fig. 3*A*) and two residues contained in Snf1 phosphorylation consensus sites (Ser^{554} and Thr^{736}). We then performed an *in vitro* kinase assay with γ-^{32}P-labeled ATP, using the purified protein as substrate and immunoprecipitated HA-tagged Snf1 and Snf1-T210A as kinases. In the presence of the WT kinase, but not in the presence of the Snf1-T210A mutant, the His_6-Cyr1(335–1066) recombinant protein incorporated ATP, demonstrating that this domain of adenylate cyclase is a *bona fide* substrate of Snf1 *in vitro* (Fig. 4*B*).

To determine which residues of His_6-Cyr1(335–1066) were phosphorylated *in vitro* by Snf1, we carried out a phosphorylation assay, followed by SDS-PAGE resolution and MS analysis. Remarkably, all the sites whose phosphorylation was Snf1-dependent *in vivo* (Fig. 3*A* and Table 3) turned out to be phosphorylated by Snf1 *in vitro* (Ser^{435}, Ser^{527}, Thr^{631}, and Ser^{645}) (Fig. 4*C* and Table 4), and among these only Ser^{435} and Ser^{527} were slightly phosphorylated in the presence of Snf1-T210A, possibly evidencing a residual activity of the mutant kinase (Table 4). Remarkably, two phosphosites that turned out to be Snf1-independent *in vivo* (Ser^{483} and Ser^{524}) and two sites that were phosphorylated upon *SNF1* deletion (Thr^{1043} and Thr^{1046}) were also found to be phosphorylated *in vitro* by Snf1 (Fig. 4*C* and Table 4). These data demonstrate that although the *in vivo* Snf1-dependent phosphosites are not contained in perfect Snf1 consensus sequences, they are potential targets of direct phosphorylation by Snf1.

Catalytic Activation of Snf1 Negatively Regulates cAMP Content—The function of adenylate cyclase is to catalyze the synthesis of cAMP, the second messenger responsible for the activation of PKA, in response to stimuli from the RAS and GPCR systems (1). Having shown that a lack of Snf1 influences the Cyr1 phosphorylation pattern and that Snf1 can phosphorylate Cyr1 *in vitro*, we wondered whether activation of Snf1 could influence the activity of adenylate cyclase. cAMP is rapidly synthesized at high levels after glucose refeeding to starved cells but is present at detectable basal levels also in exponentially growing cells (40). Therefore we measured cAMP levels in log phase cells growing in 2% glucose, either lacking Snf1 or

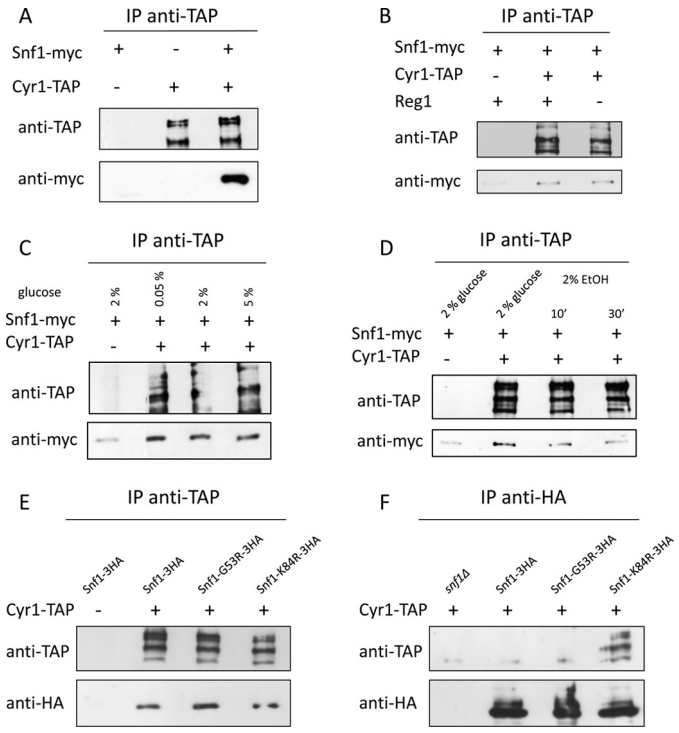

FIGURE 2. **Snf1 interacts with adenylate cyclase.** *A*, Western blot showing the detection of Snf1-myc in Cyr1-TAP immunocomplexes. *B*, Western blot showing the detection of Snf1-myc in Cyr1-TAP immunocomplexes obtained from WT and *reg1*Δ cells. *C*, Western blot showing the detection of Snf1-myc in Cyr1-TAP immunocomplexes obtained from cells in exponential phase, grown with the indicated glucose concentrations. *D*, Western blot showing the detection of Snf1-myc in Cyr1-TAP immunocomplexes obtained from cells growing in 2% glucose or shifted from medium containing 2% glucose to medium containing 2% ethanol for 10 and 30 min. *E*, Western blot showing the detection of Snf1-HA, Snf1-K84R-HA, and Snf1-G53R in Cyr1-TAP immunocomplexes. *F*, Western blot showing the detection of Cyr1-TAP in Snf1-HA, Snf1-G53R, and Snf1-K84R-HA immunocomplexes. Strains expressing untagged Snf1 or Cyr1 were used as controls. *IP*, immunoprecipitation.

harboring WT Snf1 or a Snf1-G53R mutant, which is constitutively activated because of the persistent phosphorylation of Thr^{210} (49).

Strikingly, although a lack of Snf1 did not influence the cAMP content of cells growing in glucose-repressed conditions, the presence of the Snf1-G53R mutant nearly halved the cAMP levels, as compared with the WT (Fig. 5). These data demonstrate that the catalytic activity of Snf1 can reduce the intracellular content of cAMP in glucose-repressed condition.

Catalytic Activation of Snf1 Negatively Influences PKA-dependent Transcriptional Expression—PKA regulates several cellular processes including nutrient sensing, energy metabolism, cell cycle progression, thermotolerance, osmotic shock tolerance, sporulation, pseudohyphal growth, aging, and autophagy (1). Some of these processes, such as thermotolerance, are usually used to indirectly measure the activity of the PKA pathway (8). However, Snf1 regulates these processes independently from PKA (50), and the use of these methods to measure the influence of Snf1 catalytic activity on the PKA pathway was therefore discarded.

Thus, we chose to indirectly measure the activity of the PKA pathway through the effect on the transcription of genes which are regulated by transcription factors that are PKA targets. Some transcription factors are shared downstream targets of

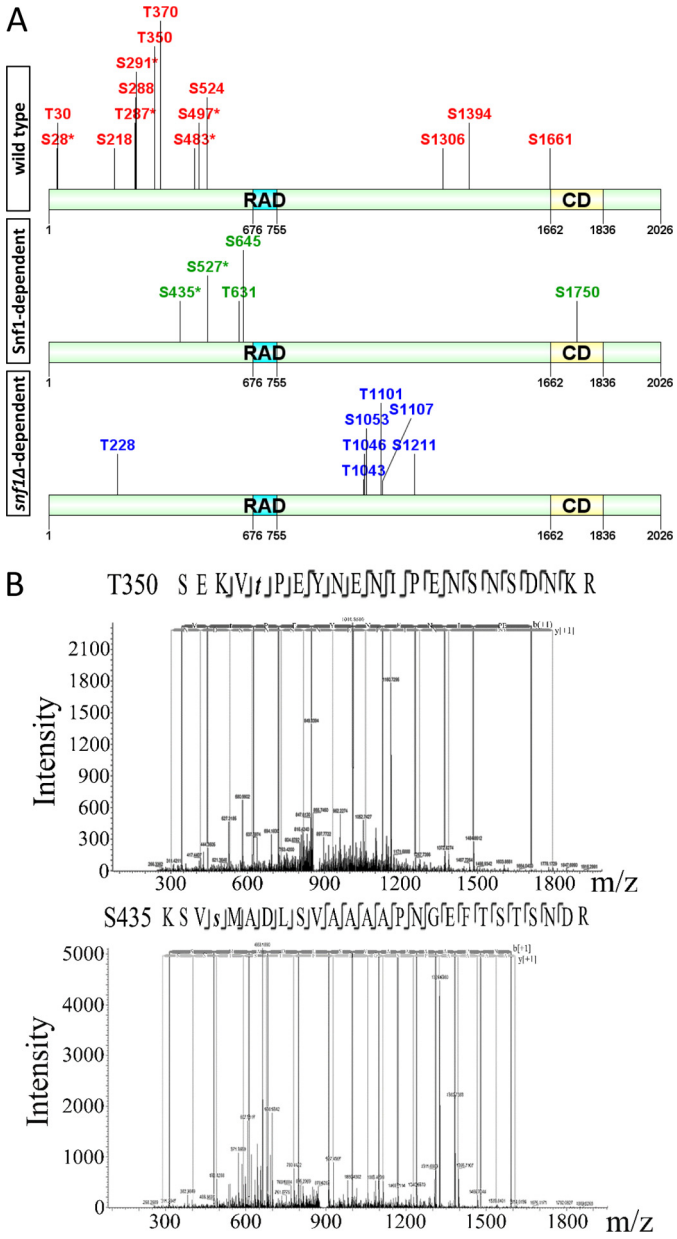

FIGURE 3. **Schematization of the Cyr1 phosphorylated sites identified *in vivo*.** *A*, graphical schematization of the phosphorylated residues identified *in vivo* by MS analysis of immunoprecipitated adenylate cyclase. Residues are divided in three subclasses: WT, if present in a WT strain and not affected by *SNF1* deletion (in *red*); Snf1-dependent, if present in a WT strain and no longer retrievable in a *snf1*Δ mutant (in *green*); and *snf1*Δ-dependent, if not present in a WT strain and only retrievable in a *snf1*Δ mutant (in *blue*). Phosphosites of each class already identified *in vivo*, as reported in PhosphoGRID, are indicated with an *asterisk*. *CD*, catalytic domain. *B*, representative fragmentation spectra of two identified phosphopeptides.

Snf1 and PKA (9, 32–36); thus the strategy required the identification of Snf1-independent target genes.

Several PKA-regulated genes have been mapped (51), and we checked the dependence of selected genes (*HXT1*, *HXT7*, and *ATR1*) during a nutritional shift-up (from ethanol to glucose containing medium) using a *cyr1*Δ*pde2*Δ*yak1*Δ strain, in which the disruption of adenylate cyclase impairs the activation of PKA (35) (Fig. 6*A*). Because *HXT1*, whose expression was PKA-dependent, is also known to be regulated by Snf1 (52), it was included in subsequent analyses as a control.

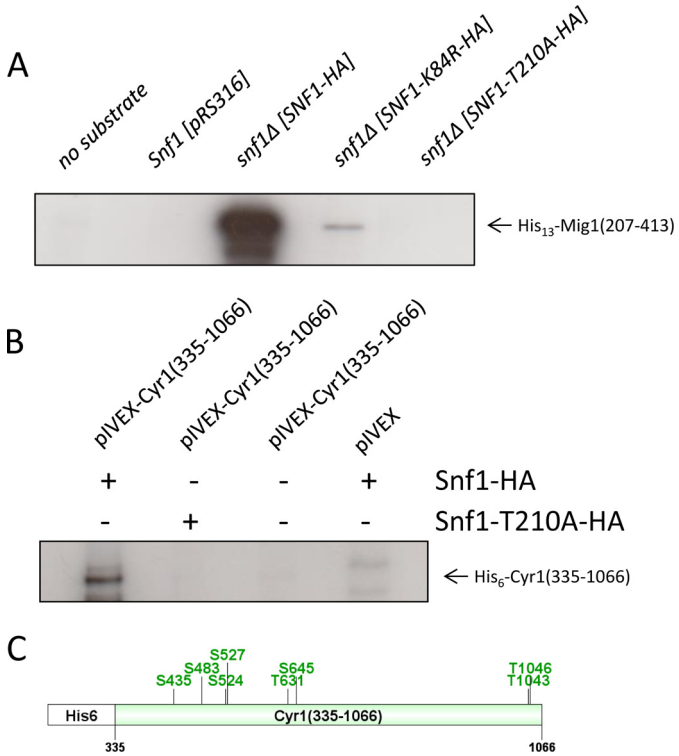

FIGURE 4. **Snf1 phosphorylates the Cyr1 RAS-associating domain *in vitro*.** *A*, autoradiography of the *in vitro* kinase assay with γ-^{32}P-labeled ATP of recombinant His_{13}-Mig1(207–413). The different lanes indicate the strain from which the kinase was immunopurified. A kinase reaction without substrate is shown as control. *B*, autoradiography of the *in vitro* kinase assay with γ-^{32}P-labeled ATP of recombinant His_6-Cyr1(335–1066). The different lanes indicate the vector contained by host *E. coli* from which purification of the substrate protein was performed. A kinase reaction without substrate is shown as control. *C*, schematization of the phosphosites identified by MS analysis on recombinant His_6-Cyr1(335–1066) after *in vitro* phosphorylation with immunopurified Snf1-HA.

TABLE 4
Cyr1(335–1066) sites phosphorylated *in vitro*

Phosphorylatable residue	Immunoprecipitated kinase			
	Snf1-HA		Snf1-T210A-HA	
	Found	Xcorr	Found	Xcorr
Thr^{370}				
Ser^{435}	×	5.98	×	3.44
Ser^{483}	×	1.84		
Ser^{497}				
Ser^{524}	×	3.57	×	1.98
Ser^{527}	×	4.06	×	1.65
Thr^{631}	×	3.24		
Ser^{645}	×	2.24		
Thr^{1043}	×	1.71		
Thr^{1046}	×	1.50		
Ser^{1053}				

To assess whether Snf1 catalytic activity influenced the expression of PKA-regulated genes, we tested the expression of *HXT1*, *HXT7*, and *ATR1* in the presence of the aforementioned Snf1-G53R mutant. *HXT1* turned out to be down-regulated in a Snf1-G53R strain grown in 2% glucose (Fig. 6*B*), thus proving that this mutant is constitutively active. The PKA-activated gene *ATR1* was slightly down-regulated in the presence of a Snf1-G53R mutant, but more strikingly, in the same strain the PKA-repressed gene *HXT7* was 5-fold derepressed (Fig. 6*B*). *HXT7* is known to be Snf1-independent (4), and we also checked its independency from the Snf1-inhibited repressor

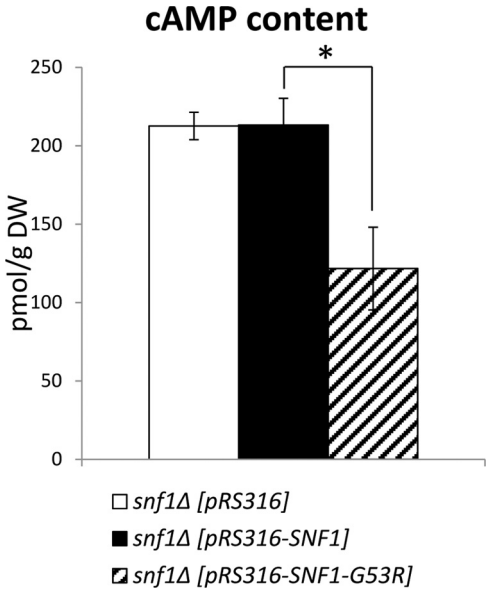

FIGURE 5. **A constitutively activated Snf1 mutant reduces intracellular cAMP levels.** Histogram showing the intracellular cAMP content of the strains expressing Snf1 or Snf1-G53R, growing in exponential phase. The data are normalized on cellular dry weight. *, p value < 0.05.

Mig1 using a *mig1*Δ strain (Fig. 6*C*), demonstrating that this gene is a useful PKA-dependent/Snf1-independent reporter gene. To further characterize the effect of Snf1 activity on PKA-dependent genes, we tested the expression of *HXT1*, *HXT7*, and *ATR1* in the presence of a Snf1-G53R mutant in 0.05, 2, and 5% glucose. In cells growing in 0.05% glucose, where PKA activity is already low and Snf1 activity is high, all three genes were equally expressed in both the WT and the Snf1-G53R strain (Fig. 6*D*). Strikingly in 5% glucose, where PKA activity should be maximal, activation of Snf1 through the G53R mutation still causes the deregulation of PKA-dependent genes (Fig. 6*D*). Altogether, these data demonstrate that Snf1 catalytic activity functionally influences the PKA pathway, determining an alteration in the expression of PKA-dependent genes.

Mutation of Snf1-dependent Phosphorylation Sites of Cyr1 Influences PKA-related Phenotypes—We showed that in the presence of active Snf1, cAMP levels were low (Fig. 5). In yeast, two phosphodiesterases, Pde1 and Pde2, degrade cAMP, and Pde1 is subjected to activation by PKA phosphorylation, generating a negative feedback on the pathway (53). Thus, to assess whether the observed effect of Snf1 on cAMP content and PKA-dependent gene expression was due to activation of the phosphodiesterases, we tested the expression of *HXT1*, *HXT7*, and *ATR1* in a *pde1*Δ*pde2*Δ strain in the presence of a Snf1-G53R mutant. Interestingly, deregulation of PKA-dependent genes by Snf1 activation was observed even in the absence of the phosphodiesterases (Fig. 7*A*). Only the derepression of *HXT7* was somehow reduced, but the basal levels of the mRNA were already high in the *pde1*Δ*pde2*Δ strain compared with a WT (data not shown).

We therefore tested the possibility that the PKA transcriptional activity was instead dependent upon phosphorylation of adenylate cyclase. Thus, we generated a mutant Cyr1 in which the four Snf1-dependent phosphosites near the RAD (Ser^{435}, Ser^{527}, Thr^{631}, and Ser^{645}), identified *in vivo* (Fig. 3*A* and Table

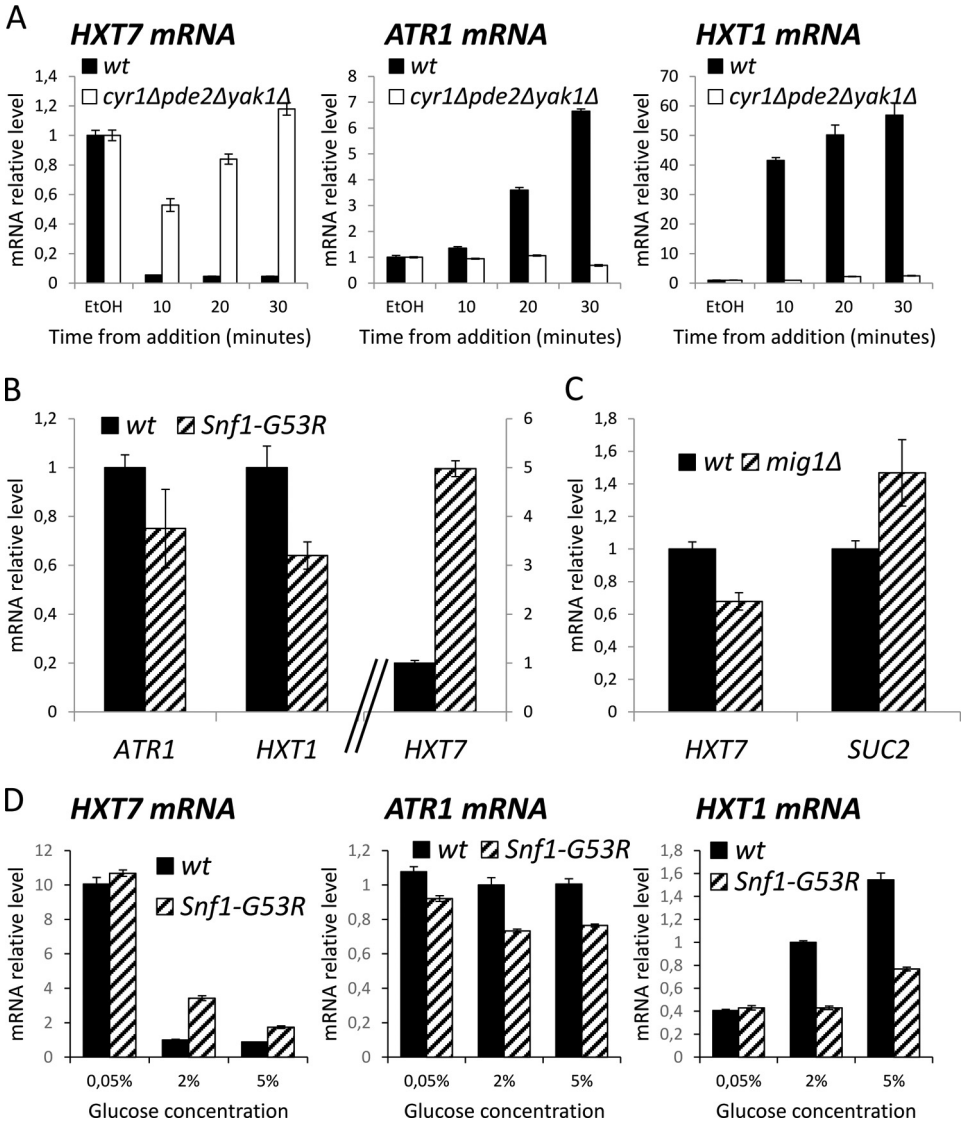

FIGURE 6. **Expression of PKA-dependent genes in the presence of constitutively activated Snf1.** *A*, real time PCR quantification of mRNAs of the indicated genes in cells in exponential phase of growth in 2% ethanol and after addition of 5% glucose (final concentration). *B*, real time PCR quantification of mRNAs of the indicated genes in cells expressing Snf1 or Snf1-G53R in exponential phase of growth in 2% glucose. *C*, real time PCR quantification of mRNAs of the indicated genes in WT and *mig1*Δ cells in exponential phase of growth in 2% glucose. *D*, real time PCR quantification of mRNAs of the indicated genes in cells in exponential phase of growth in 0.05% glucose, 2% glucose, or 5% glucose.

3) and confirmed to be Snf1 targets *in vitro* (Fig. 4*C* and Table 4), were mutated to glutamate to mimic constitutive phosphorylation. The resulting mutant, Cyr1-4E, had no effect on duplication time (WT 117 ± 12 min, Cyr1-4E 134 ± 5 min), cell volume (WT 58.8 ± 0.8 fL, Cyr1-4E 58.3 ± 1.1 fL) and protein content (WT 400 ± 40 a.u., Cyr1-4E 417 ± 37 a.u.). Although the mutant protein was expressed at the same level as WT Cyr1 (Fig. 7*B*), it induced, in a *cyr1*Δ*pde2*Δ*yak1*Δ background, a higher resistance to heat shock (Fig. 7*C*), a typical hallmark of PKA activity impairment (54). Furthermore, we tested the expression of *HXT7* in a Cyr1-4E mutant compared with the WT. Interestingly, we observed a more than 2-fold derepression of *HXT7* in the presence of the mutated Cyr1, indicating a partial down-regulation of the pathway (Fig. 7*D*).

Taken together, these data indicate that Cyr1 phosphorylation, rather than phosphodiesterase activation, is important for the control of *HXT7* expression. In particular, the phosphorylation status of four Snf1-dependent residues seems to directly influence PKA activity.

Discussion

A major challenge in the understanding of a signaling pathway is the discovery of cross-talk with other pathways. Because Snf1 is mainly known for its role in shaping metabolism to guarantee cell growth in nutritional scarceness, it seemed likely that it could regulate other signaling pathways that cause opposite outcomes. In search for new targets of Snf1, we identified a set of previously unknown Snf1-interacting proteins (Fig. 1 and Table 2), including adenylate cyclase (Cyr1), suggesting a possible cross-talk between Snf1 and PKA pathways. PKA was a possible candidate as a Snf1-regulated pathway, because it is activated in conditions of nutrient abundance. The two pathways share common downstream targets, such as transcription factor Adr1 (9, 33–36), and PKA has been reported to regulate

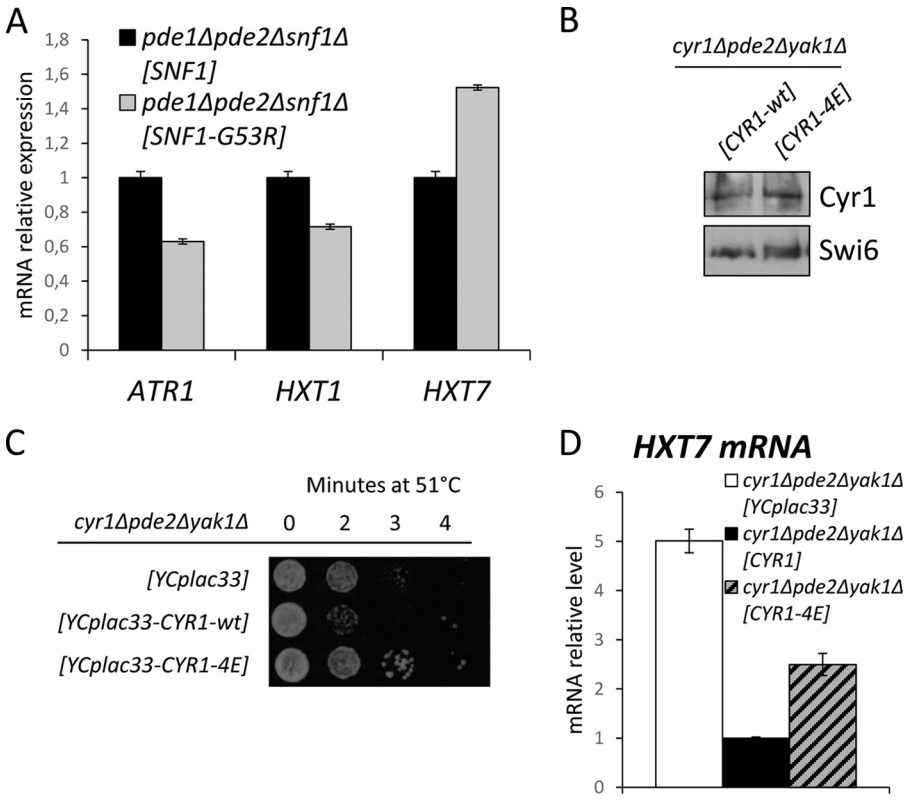

FIGURE 7. **Mutation of Snf1-dependent phosphorylation sites in the Cyr1 RAD affects PKA-dependent transcription.** *A*, real time PCR quantification of mRNAs of the indicated genes in *pde1Δpde2Δsnf1Δ* cells expressing Snf1 or Snf1-G53R in exponential phase of growth in 2% glucose. *B*, Western blot showing the detection of Cyr1 in the *cyr1Δpde2Δyak1Δ* strain transformed with the indicated plasmid. Swi6 was used as loading control. *C*, drop test on YPD plates of 10^4 cells of the *cyr1Δpde2Δyak1Δ* strain transformed with the indicated plasmid after heat shock at 51 °C for the indicated time. *D*, real time PCR quantification of *HXT7* mRNA in *cyr1Δpde2Δyak1Δ* cells transformed with the indicated plasmid in exponential phase of growth in 2% glucose.

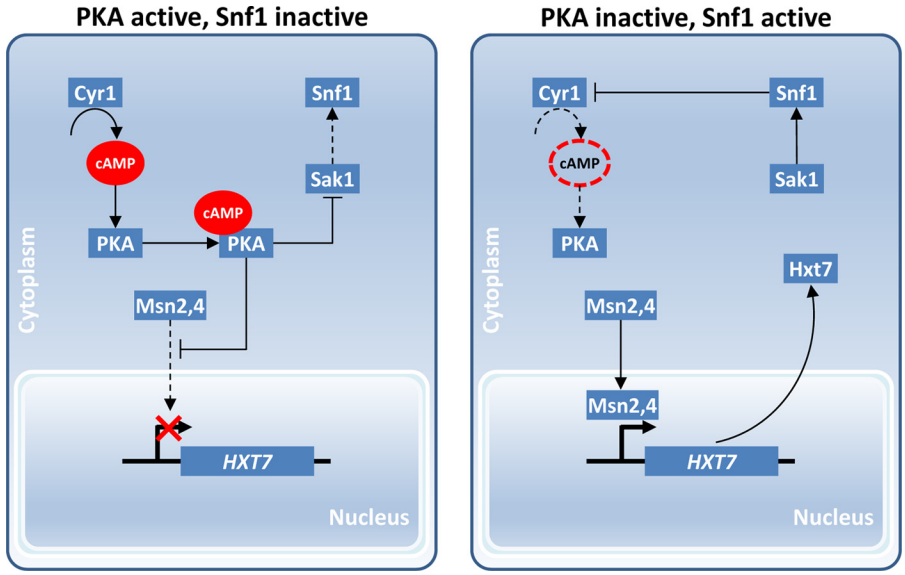

FIGURE 8. **Map of the cross-talk between the Snf1 and PKA pathways.** Schematization of the basic circuitry of the cross-talk between the Snf1 and PKA pathway, applied to the expression of the PKA-repressed gene *HXT7*. Subsidiary pathways were omitted for simplification. *Dotted lines* and *solid lines* indicate inefficient and efficient processes respectively. In high glucose condition, Cyr1 produces high cAMP levels, which activate PKA that can inhibit Msn2,4 translocation into the nucleus and Sak1 activity. Therefore, expression of *HXT7* is low and Sak1 inefficiently phosphorylates Snf1. In low glucose, Snf1 is active and inhibits Cyr1, thus resulting in lower cAMP levels and lower PKA activity; Msn2,4 is nuclear and activates *HXT7* expression.

the recruitment of Snf1 to the vacuole and to contribute to the inactivation of the Snf1-activating kinase Sak1 (31, 32). This regulation seem to be evolutionarily conserved, because in mammalian cells PKA phosphorylates and inactivates the Snf1 orthologue AMPK (37). Thus, showing the converse regulation of the PKA pathway by Snf1, we suggest a novel cross-talk mechanism. Although we showed that the interaction of Snf1 and Cyr1 is independent from nutritional conditions (Fig. 2, *C* and *D*) and from Snf1 activity (Fig. 2, *E* and *F*), we demonstrated that the lack of Snf1 could alter the phosphorylation status of

Cyr1 *in vivo* and that Snf1 can phosphorylate an important regulatory domain of adenylate cyclase *in vitro* (Figs. 3 and 4*B*). Moreover, by mapping the *in vitro* phosphorylated sites, we demonstrated that Snf1 directly phosphorylates the phosphosites, which turned out to be Snf1-dependent *in vivo* (Fig. 4*C* and Table 4). Strikingly, by using a constitutively activated Snf1 mutant, we highlighted an inverse correlation between the activation state of the kinase and the intracellular content of cAMP (Fig. 5). To determine whether the activity of Snf1 had actual influence on PKA activity, we established a method based on the expression of an endogenous gene used as a reporter. The gene *HXT7*, identified as a target of the PKA-repressed transcription factors Msn2 and Msn4 (51), was chosen for this purpose. In fact, it showed PKA-dependent repression in a strain lacking adenylate cyclase (Fig. 6*A*), and it was independent from direct Snf1 activity in a *mig1*Δ strain (Fig. 6*C*). Moreover, *HXT7* was already reported to be Snf1-independent (4), and no interaction of Snf1-regulated transcription factors with the promoter of *HXT7* was reported in specialized databases. *HXT7* turned out to be dramatically derepressed in a Snf1-G53R strain (Fig. 6*B*), thus linking Snf1 activation to the transcription of PKA-dependent genes. Moreover, the phosphomimetic mutation of Snf1-dependent Cyr1 phosphosites induced alteration of heat shock resistance and caused *HXT7* derepression. *HXT7* encodes for a high affinity glucose transporter, specifically expressed in low glucose media (55), and the dependence of its expression from an interplay between PKA and Snf1, which act as opposite pathways, seems therefore biologically consistent. The regulation of PKA pathway by Snf1 seems likely to occur in nutrient limiting conditions, but the study in glucose abundant medium allowed the use of the otherwise lethal mutant *snf1*Δ and the activated mutant Snf1-G53R in the absence of a high basal activity of Snf1. Altogether, these findings (summarized in Fig. 8) added a new link in the circuitry involving these two major signaling pathways, with Snf1 regulating both directly and indirectly the content of cAMP and thus the activation state of PKA, consequently enhancing the expression of genes required in conditions of nutrient scarceness and stress.

Author Contributions—R. N. performed experiments, analyzed data, and wrote the paper. F. T., M. G., A. C., V. R., and S. N. performed experiments and analyzed data. G. T. and P. C. analyzed data and wrote the paper.

Acknowledgments—We thank M. C. Schmidt for the generous gift of the pH_{13}-MIG1 plasmid, J. Thevelein for the pde1Δpde2Δ strain, and L. Breeden for anti-Swi6 antibody.

References

1. Santangelo, G. M. (2006) Glucose signaling in *Saccharomyces cerevisiae*. *Microbiol. Mol. Biol. Rev.* **70,** 253–282
2. Broach, J. R. (2012) Nutritional control of growth and development in yeast. *Genetics* **192,** 73–105
3. Busti, S., Coccetti, P., Alberghina, L., and Vanoni, M. (2010) Glucose signaling-mediated coordination of cell growth and cell cycle in *Saccharomyces cerevisiae*. *Sensors* **10,** 6195–6240
4. Zaman, S., Lippman, S. I., Schneper, L., Slonim, N., and Broach, J. R. (2009) Glucose regulates transcription in yeast through a network of signaling pathways. *Mol. Syst. Biol.* **5,** 245
5. Alberghina, L., Mavelli, G., Drovandi, G., Palumbo, P., Pessina, S., Tripodi, F., Coccetti, P., and Vanoni, M. (2012) Cell growth and cell cycle in *Saccharomyces cerevisiae*: basic regulatory design and protein-protein interaction network. *Biotechnol. Adv.* **30,** 52–72
6. Tripodi, F., Nicastro, R., Reghellin, V., and Coccetti, P. (2015) Post-translational modifications on yeast carbon metabolism: Regulatory mechanisms beyond transcriptional control. *Biochim. Biophys. Acta* **1850,** 620–627
7. Thevelein, J. M., and de Winde, J. H. (1999) Novel sensing mechanisms and targets for the cAMP-protein kinase A pathway in the yeast *Saccharomyces cerevisiae*. *Mol. Microbiol.* **33,** 904–918
8. Toda, T., Cameron, S., Sass, P., Zoller, M., Scott, J. D., McMullen, B., Hurwitz, M., Krebs, E. G., and Wigler, M. (1987) Cloning and characterization of BCY1, a locus encoding a regulatory subunit of the cyclic AMP-dependent protein kinase in *Saccharomyces cerevisiae*. *Mol. Cell. Biol.* **7,** 1371–1377
9. Görner, W., Durchschlag, E., Martinez-Pastor, M. T., Estruch, F., Ammerer, G., Hamilton, B., Ruis, H., and Schüller, C. (1998) Nuclear localization of the C_2H_2 zinc finger protein Msn2p is regulated by stress and protein kinase A activity. *Genes Dev.* **12,** 586–597
10. Gasch, A. P., Spellman, P. T., Kao, C. M., Carmel-Harel, O., Eisen, M. B., Storz, G., Botstein, D., and Brown, P. O. (2000) Genomic expression programs in the response of yeast cells to environmental changes. *Mol. Biol. Cell.* **11,** 4241–4257
11. Wei, M., Fabrizio, P., Hu, J., Ge, H., Cheng, C., Li, L., and Longo, V. D. (2008) Life span extension by calorie restriction depends on Rim15 and transcription factors downstream of Ras/PKA, Tor, and Sch9. *PLoS Genet.* **4,** e13
12. Klein, C., and Struhl, K. (1994) Protein kinase A mediates growth-regulated expression of yeast ribosomal protein genes by modulating RAP1 transcriptional activity. *Mol. Cell. Biol.* **14,** 1920–1928
13. Cytryńska, M., Frajnt, M., and Jakubowicz, T. (2001) *Saccharomyces cerevisiae* pyruvate kinase Pyk1 is PKA phosphorylation substrate *in vitro*. *FEMS Microbiol. Lett.* **203,** 223–227
14. Portela, P., Howell, S., Moreno, S., and Rossi, S. (2002) *In vivo* and *in vitro* phosphorylation of two isoforms of yeast pyruvate kinase by protein kinase A. *J. Biol. Chem.* **277,** 30477–30487
15. Portela, P., Moreno, S., and Rossi, S. (2006) Characterization of yeast pyruvate kinase 1 as a protein kinase A substrate, and specificity of the phosphorylation site sequence in the whole protein. *Biochem. J.* **396,** 117–126
16. Hedbacker, K., and Carlson, M. (2008) SNF1/AMPK pathways in yeast. *Front. Biosci.* **13,** 2408–2420
17. Hardie, D. G. (2007) AMP-activated/SNF1 protein kinases: conserved guardians of cellular energy. *Nat. Rev. Mol. Cell Biol.* **8,** 774–785
18. Hong, S.-P., Leiper, F. C., Woods, A., Carling, D., and Carlson, M. (2003) Activation of yeast Snf1 and mammalian AMP-activated protein kinase by upstream kinases. *Proc. Natl. Acad. Sci. U.S.A.* **100,** 8839–8843
19. Sutherland, C. M., Hawley, S. A., McCartney, R. R., Leech, A., Stark, M. J., Schmidt, M. C., and Hardie, D. G. (2003) Elm1p is one of three upstream kinases for the *Saccharomyces cerevisiae* SNF1 complex. *Curr. Biol.* **13,** 1299–1305
20. Ludin, K., Jiang, R., and Carlson, M. (1998) Glucose-regulated interaction of a regulatory subunit of protein phosphatase 1 with the Snf1 protein kinase in *Saccharomyces cerevisiae*. *Proc. Natl. Acad. Sci. U.S.A.* **95,** 6245–6250
21. Sanz, P., Alms, G. R., Haystead, T. A., and Carlson, M. (2000) Regulatory interactions between the Reg1-Glc7 protein phosphatase and the Snf1 protein kinase. *Mol. Cell. Biol.* **20,** 1321–1328
22. Pessina, S., Tsiarentsyeva, V., Busnelli, S., Vanoni, M., Alberghina, L., and Coccetti, P. (2010) Snf1/AMPK promotes S-phase entrance by controlling CLB5 transcription in budding yeast. *Cell Cycle.* **9,** 2189–2200
23. Busnelli, S., Tripodi, F., Nicastro, R., Cirulli, C., Tedeschi, G., Pagliarin, R., Alberghina, L., and Coccetti, P. (2013) Snf1/AMPK promotes SBF and MBF-dependent transcription in budding yeast. *Biochim. Biophys. Acta* **1833,** 3254–3264
24. Braun, K. A., Vaga, S., Dombek, K. M., Fang, F., Palmisano, S., Aebersold, R., and Young, E. T. (2014) Phosphoproteomic analysis identifies proteins

involved in transcription-coupled mRNA decay as targets of Snf1 signaling. *Sci. Signal.* **7,** ra64
25. Nicastro, R., Tripodi, F., Guzzi, C., Reghellin, V., Khoomrung, S., Capusoni, C., Compagno, C., Airoldi, C., Nielsen, J., Alberghina, L., and Coccetti, P. (2015) Enhanced amino acid utilization sustains growth of cells lacking Snf1/AMPK. *Biochim. Biophys. Acta* **1853,** 1615–1625
26. Young, E. T., Zhang, C., Shokat, K. M., Parua, P. K., and Braun, K. A. (2012) The AMP-activated protein kinase Snf1 regulates transcription factor binding, RNA polymerase II activity and mRNA stability of glucose-repressed genes in *Saccharomyces cerevisiae*. *J. Biol. Chem.* **287,** 29021–29034
27. Nehlin, J. O., and Ronne, H. (1990) Yeast MIG1 repressor is related to the mammalian early growth response and Wilms' tumour finger proteins. *EMBO J.* **9,** 2891–2898
28. Vincent, O., and Carlson, M. (1998) Sip4, a Snf1 kinase-dependent transcriptional activator, binds to the carbon source-responsive element of gluconeogenic genes. *EMBO J.* **17,** 7002–7008
29. Lesage, P., Yang, X., and Carlson, M. (1996) Yeast SNF1 protein kinase interacts with SIP4, a C6 zinc cluster transcriptional activator: a new role for SNF1 in the glucose response. *Mol. Cell. Biol.* **16,** 1921–1928
30. Randez-Gil, F., Bojunga, N., Proft, M., and Entian, K. D. (1997) Glucose derepression of gluconeogenic enzymes in *Saccharomyces cerevisiae* correlates with phosphorylation of the gene activator Cat8p. *Mol. Cell. Biol.* **17,** 2502–2510
31. Barrett, L., Orlova, M., Maziarz, M., and Kuchin, S. (2012) Protein kinase A contributes to the negative control of Snf1 protein kinase in *Saccharomyces cerevisiae*. *Eukaryot. Cell.* **11,** 119–128
32. Hedbacker, K., Townley, R., and Carlson, M. (2004) Cyclic AMP-dependent protein kinase regulates the subcellular localization of Snf1-Sip1 protein kinase. *Mol. Cell. Biol.* **24,** 1836–1843
33. Cherry, J. R., Johnson, T. R., Dollard, C., Shuster, J. R., and Denis, C. L. (1989) Cyclic AMP-dependent protein kinase phosphorylates and inactivates the yeast transcriptional activator ADR1. *Cell.* **56,** 409–419
34. Ratnakumar, S., Kacherovsky, N., Arms, E., and Young, E. T. (2009) Snf1 controls the activity of Adr1 through dephosphorylation of Ser230. *Genetics* **182,** 735–745
35. Görner, W., Durchschlag, E., Wolf, J., Brown, E. L., Ammerer, G., Ruis, H., and Schüller, C. (2002) Acute glucose starvation activates the nuclear localization signal of a stress-specific yeast transcription factor. *EMBO J.* **21,** 135–144
36. De Wever, V., Reiter, W., Ballarini, A., Ammerer, G., and Brocard, C. (2005) A dual role for PP1 in shaping the Msn2-dependent transcriptional response to glucose starvation. *EMBO J.* **24,** 4115–4123
37. Djouder, N., Tuerk, R. D., Suter, M., Salvioni, P., Thali, R. F., Scholz, R., Vaahtomeri, K., Auchli, Y., Rechsteiner, H., Brunisholz, R. A., Viollet, B., Mäkelä, T. P., Wallimann, T., Neumann, D., and Krek, W. (2010) PKA phosphorylates and inactivates AMPKα to promote efficient lipolysis. *EMBO J.* **29,** 469–481
38. Vanhalewyn, M., Dumortier, F., Debast, G., Colombo, S., Ma, P., Winderickx, J., Van Dijck, P., and Thevelein, J. M. (1999) A mutation in *Saccharomyces cerevisiae* adenylate cyclase, Cyr1K1876M, specifically affects glucose- and acidification-induced cAMP signalling and not the basal cAMP level. *Mol. Microbiol.* **33,** 363–376
39. Chandrashekarappa, D. G., McCartney, R. R., and Schmidt, M. C. (2013) Ligand binding to the AMP-activated protein kinase active site mediates protection of the activation loop from dephosphorylation. *J. Biol. Chem.* **288,** 89–98
40. Petkova, M. I., Pujol-Carrion, N., Arroyo, J., García-Cantalejo, J., and Angeles de la Torre-Ruiz, M. (2010) Mtl1 is required to activate general stress response through Tor1 and Ras2 inhibition under conditions of glucose starvation and oxidative stress. *J. Biol. Chem.* **285,** 19521–31
41. Collins, S. R., Kemmeren, P., Zhao, X.-C., Greenblatt, J. F., Spencer, F., Holstege, F. C., Weissman, J. S., and Krogan, N. J. (2007) Toward a comprehensive atlas of the physical interactome of *Saccharomyces cerevisiae*. *Mol. Cell. Proteomics* **6,** 439–450
42. Krogan, N. J., Cagney, G., Yu, H., Zhong, G., Guo, X., Ignatchenko, A., Li, J., Pu, S., Datta, N., Tikuisis, A. P., Punna, T., Peregrín-Alvarez, J. M., Shales, M., Zhang, X., Davey, M., Robinson, M. D., Paccanaro, A., Bray, J. E., Sheung, A., Beattie, B., Richards, D. P., Canadien, V., Lalev, A., Mena, F., Wong, P., Starostine, A., Canete, M. M., Vlasblom, J., Wu, S., Orsi, C., Collins, S. R., Chandran, S., Haw, R., Rilstone, J. J., Gandi, K., Thompson, N. J., Musso, G., St Onge, P., Ghanny, S., Lam, M. H., Butland, G., Altaf-Ul, A. M., Kanaya, S., Shilatifard, A., O'Shea, E., Weissman, J. S., Ingles, C. J., Hughes, T. R., Parkinson, J., Gerstein, M., Wodak, S. J., Emili, A., and Greenblatt, J. F. (2006) Global landscape of protein complexes in the yeast *Saccharomyces cerevisiae*. *Nature* **440,** 637–643
43. Breitkreutz, A., Choi, H., Sharom, J. R., Boucher, L., Neduva, V., Larsen, B., Lin, Z.-Y., Breitkreutz, B.-J., Stark, C., Liu, G., Ahn, J., Dewar-Darch, D., Reguly, T., Tang, X., Almeida, R., Qin, Z. S., Pawson, T., Gingras, A.-C., Nesvizhskii, A. I., and Tyers, M. (2010) A global protein kinase and phosphatase interaction network in yeast. *Science* **328,** 1043–1046
44. Treitel, M. A., Kuchin, S., and Carlson, M. (1998) Snf1 protein kinase regulates phosphorylation of the Mig1 repressor in *Saccharomyces cerevisiae*. *Mol. Cell. Biol.* **18,** 6273–6280
45. Smolka, M. B., Albuquerque, C. P., Chen, S. H., and Zhou, H. (2007) Proteome-wide identification of *in vivo* targets of DNA damage checkpoint kinases. *Proc. Natl. Acad. Sci. U.S.A.* **104,** 10364–10369
46. Holt, L. J., Tuch, B. B., Villén, J., Johnson, A. D., Gygi, S. P., and Morgan, D. O. (2009) Global analysis of Cdk1 substrate phosphorylation sites provides insights into evolution. *Science* **325,** 1682–1686
47. Li, X., Gerber, S. A., Rudner, A. D., Beausoleil, S. A., Haas, W., Villén, J., Elias, J. E., and Gygi, S. P. (2007) Large-scale phosphorylation analysis of α-factor-arrested *Saccharomyces cerevisiae*. *J. Proteome Res.* **6,** 1190–1197
48. Gruhler, A., Olsen, J. V., Mohammed, S., Mortensen, P., Faergeman, N. J., Mann, M., and Jensen, O. N. (2005) Quantitative phosphoproteomics applied to the yeast pheromone signaling pathway. *Mol. Cell. Proteomics* **4,** 310–327
49. Estruch, F., Treitel, M. A., Yang, X., and Carlson, M. (1992) N-terminal mutations modulate yeast SNF1 protein kinase function. *Genetics* **132,** 639–650
50. Hong, S.-P., and Carlson, M. (2007) Regulation of snf1 protein kinase in response to environmental stress. *J. Biol. Chem.* **282,** 16838–16845
51. Livas, D., Almering, M. J., Daran, J.-M., Pronk, J. T., and Gancedo, J. M. (2011) Transcriptional responses to glucose in *Saccharomyces cerevisiae* strains lacking a functional protein kinase A. *BMC Genomics* **12,** 405
52. Tomás-Cobos, L., and Sanz, P. (2002) Active Snf1 protein kinase inhibits expression of the *Saccharomyces cerevisiae* HXT1 glucose transporter gene. *Biochem. J.* **368,** 657–663
53. Ma, P., Wera, S., Van Dijck, P., and Thevelein, J. M. (1999) The PDE1-encoded low-affinity phosphodiesterase in the yeast *Saccharomyces cerevisiae* has a specific function in controlling agonist-induced cAMP signaling. *Mol. Biol. Cell.* **10,** 91–104
54. Belotti, F., Tisi, R., Paiardi, C., Groppi, S., and Martegani, E. (2011) PKA-dependent regulation of Cdc25 RasGEF localization in budding yeast. *FEBS Lett.* **585,** 3914–3920
55. Reifenberger, E., Freidel, K., and Ciriacy, M. (1995) Identification of novel HXT genes in *Saccharomyces cerevisiae* reveals the impact of individual hexose transporters on glycolytic flux. *Mol. Microbiol.* **16,** 157–167
56. Van de Velde, S., and Thevelein, J. M. (2008) Cyclic AMP-protein kinase A and Snf1 signaling mechanisms underlie the superior potency of sucrose for induction of filamentation in *Saccharomyces cerevisiae*. *Eukaryot. Cell* **7,** 286–293